

# Investigating Groundwater Flow in Alluvium in the Upper Nueces River Basin, Texas

CE394K GIS in Water Resources  
Term Project Report  
Fall 2017



**Caroline Hackett**  
**MS Hydrogeology 2018**  
**Jackson School of Geosciences**

 **TEXAS** Geosciences  
The University of Texas at Austin  
Jackson School of Geosciences

## **Introduction**

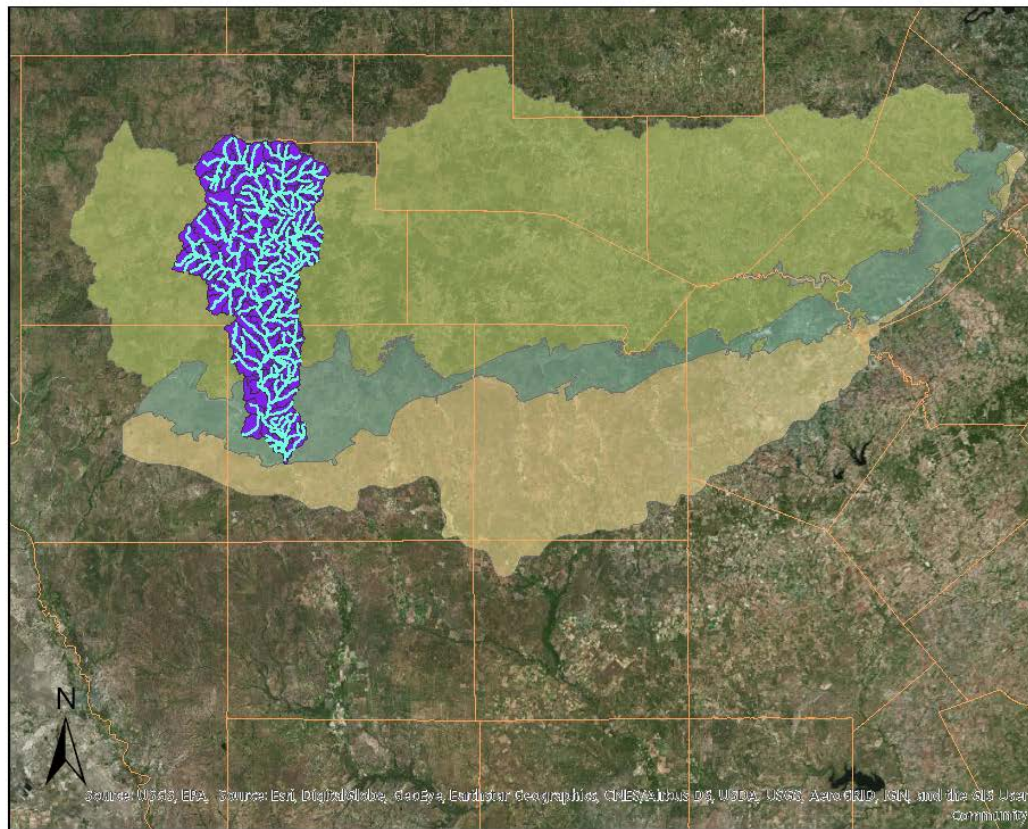
Quantification of surface water-groundwater interactions has gained attention in recent decades (Fleckenstein et al., 2010), enhanced by strides in modeling capabilities and the integration of geographic information systems (GIS) (Kresic and Mikszewski, 2013). Models such as GSFLOW, HEC-HMS, MODFLOW, VarKarst-R, Community Land Model, and WetSpa are used to estimate stream-groundwater interactions and distributed recharge in karst landscapes. These models have been used to study attenuation of floods and flood effects on alluvial groundwater levels (Bailly-Comte et al., 2012, Bernard-Jannin et al., 2016). Batelaan et al. (2007) demonstrated that a GIS-based, conceptual water balance model can be coupled with a regional groundwater model to accurately simulate distributed recharge. GIS-based modeling can also be used to estimate water storage reservoirs using distributed elevation, climate, hydrologic, and land cover data (Chenini and Mammou, 2010 and Graf and Przybyłek, 2014). Green et al. (2008) used geophysical surveys to estimate the lateral and vertical extent of alluvium in the Leona River basin in Texas and performed aquifer tests to determine hydraulic conductivity, which were used to estimate the discharge from the Leona River floodplain. Subsurface karst conduits within karstic floodplains have been modeled in various ways, including using porous medium Darcy flow (Chen et al., 2013); with an epikarst reservoir serving as a production and routing store (Jukić and Denić-Jukić, 2009); and by a groundwater recharge parameter dependent on river discharge (Zampieri et al., 2012).

This study estimates shallow groundwater storage and transport within the alluvial floodplain. The role of alluvial deposits overlying karstic carbonate river beds in the floodplain water balance is not well understood. However, alluvium can be a significant source of storage and transmission of river underflow and the site of hyporheic exchange between surface and groundwater. Alluvium plays a role in attenuation of flood pulses in karst basins, and it may buffer recharge into the underlying aquifer through discrete karst recharge features (swallets, faults, conduits, etc.). Alternatively, river water storage in alluvium may shift or extend the time over which recharge to those discrete karst features can occur, thereby enhancing recharge.

In Texas, the Brazos River Alluvial Aquifer is the only alluvial aquifer designated by the state as a minor aquifer, though shallow groundwater adjacent to most major Texas rivers are becoming locally significant for water supply. Many of the basins on the Edwards Plateau in south-central Texas have extensive alluvium in the upstream reaches, composed of the Pleistocene-age Leona Formation, the Holocene-age Uvalde Gravels, and Quaternary deposits, consisting of mostly chert and limestone cobbles. These areas are conceptualized as ‘floodplain conveyance systems’, where river water and shallow groundwater flow through alluvium deposits and older alluvial terraces. Quantification of groundwater storage in alluvium is critical, as discrete recharge to the Edwards Aquifer from the streambed must be carefully estimated for optimal resource management and groundwater permitting (Hauwert, 2016).

The Nueces River basin is the largest contributor of recharge to the Edwards Aquifer, and recent studies suggest that areas in the Edwards Aquifer Contributing Zone supply autogenic and allogenic recharge, with inter-aquifer flow possible (Figure 1). The river underflow and shallow groundwater stored and transmitted in alluvial deposits and terraces may become an important source of river discharge in low flow conditions and thus recharge to the Edwards and Trinity aquifers (Figure 2). In this study, I investigate shallow groundwater flow in alluvial floodplain deposits of the Nueces headwaters. Ultimately, the results of this project will help to quantify the role of alluvium in buffering discrete infiltration into karst features and/or promoting recharge.

## Edwards Aquifer Zones and Nueces River Headwaters



0 5 10 20 30 40  
Miles



- Nueces HW Flowline
- Nueces HW Catchments
- USA Counties**
- USA\_Counties
- AquiferZones**
- Symbolize**
- Drainage Area
- Recharge Zone
- Artesian Zone

*Figure 1.* Extent of the Edwards Aquifer in south-central Texas. The Nueces River headwaters stretch from the Nueces canyon country in the north to the southern extent of the Edwards Aquifer Recharge Zone. The Nueces basin is a significant contributor of discrete recharge to the Edwards Aquifer, as surface water infiltrates through karst features, fractures, and faults in the riverbed. Alluvium in the floodplain may buffer or enhance these discrete recharge pathways.

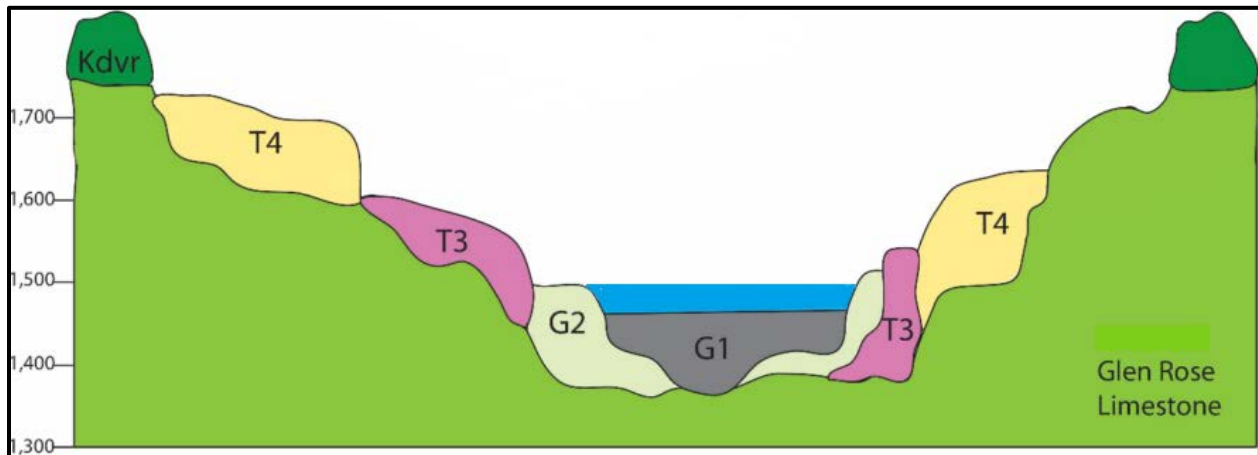


*Figure 2.* Alluvial deposits and terraces in the Nueces River floodplain act as a floodplain conveyance system in combination with river flow and shallow groundwater. The floodplain is underlain by Glen Rose Limestone, which is part of the Trinity Aquifer and also a contributor to Edwards Aquifer recharge, called interformational flow. The Devils River Limestone (Kdvr) is part of the younger Edwards Group. Elevations are in feet.

### **Objectives**

The objective of this project is to use ArcGIS Pro to model the magnitude and direction of groundwater flow through alluvial deposits in the upper Nueces River basin. The values generated from this analysis in ArcGIS Pro are compared to calculated subsurface velocities resulting from dye tracer testing conducted on the Nueces River in spring and summer 2017.

### **Methods**

The Darcy Flow tool is used to calculate subsurface flow magnitude and direction. Darcy's Law describes flow in a porous medium. The Darcy velocity,  $q$  [L/T], is proportional to the hydraulic conductivity,  $K$  [L/T], and the hydraulic head gradient [unitless]:

$$q = -K * \nabla h$$

The Darcy Flow tool produces the following outputs:

1. *Flow direction raster:* each cell value represents the direction of the seepage velocity vector at the center of the cell. It is the average of the seepage velocities through the four cell faces. The seepage velocity is the average linear velocity of the groundwater, which is equal to the Darcy velocity, also called specific discharge ( $q$ ), divided by the effective porosity.
2. *Flow magnitude raster:* each cell value represents the magnitude of the seepage velocity at the center of the cell, calculated as the average of the velocity through the four cell faces.
3. *Volume balance residual raster:* each cell value represents the groundwater volume balance residual in the cell, as determined with Darcy's Law. Low values indicate a reasonable estimation of groundwater flow.



The Darcy Flow geoprocessing tool requires the following four inputs, which must have the same size cells:

1. *Groundwater head elevation raster*: each cell value represents the groundwater elevation at that location. [m]
2. *Saturated thickness raster*: each cell value represents the thickness of saturated alluvium from the water table down to the limestone bedrock. [m]
3. *Transmissivity raster*: each cell value represents the transmissivity of the alluvium at that location. Transmissivity,  $T$  [ $m^2/s$ ], is equal to the hydraulic conductivity ( $K$ ) multiplied by the saturated thickness ( $b$ ):

$$T = K * b$$

4. *Porosity raster*: each cell value represents the effective porosity of the alluvium at the location. [unitless]

Groundwater head elevation was determined using the Spline tool to interpolate between the annual average groundwater levels in four monitoring wells maintained by the Edwards Aquifer Authority and the Texas Water Development Board (Figure 3). The general trend is decreasing groundwater head towards the southeast, which agrees with the regional groundwater flowpaths in this portion of the Edwards Plateau.

### Groundwater Head Elevation Raster

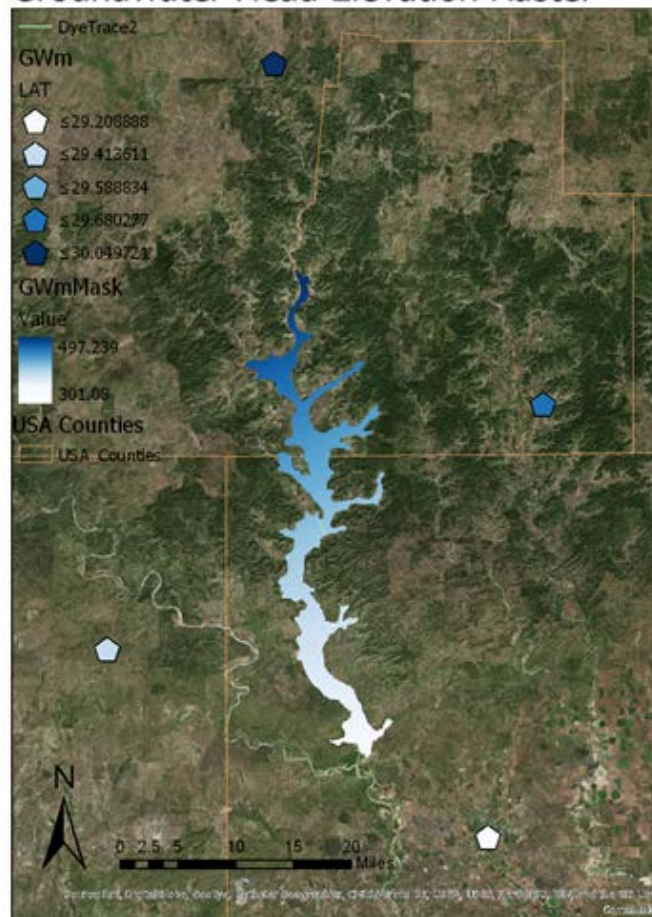


Figure 3. Groundwater head elevations interpolated from the four available monitoring wells.

The saturated thickness raster is a key input into the Darcy Flow tool, however, well log data are extremely limited in the alluvial terraces of the upper Nueces River. Several attempts were made to determine the saturated thickness based on well logs that are publicly available through the Texas Water Development Board's online groundwater database. Using the depth to bedrock and depth to water recorded on the well driller's logs, the saturated thickness can be calculated as:

$$b = [\text{well surface elevation} - \text{depth to groundwater}] - \text{bedrock elevation}$$

This approach was complicated by several factors, however. Depth to bedrock and depth to water were only available on a fraction of the available well logs, and the accuracy of the depth to bedrock is questionable in many cases. Importantly, this approach is only applicable when the water table is above the elevation of bedrock (Glen Rose limestone), which occurs where the bedrock has been incised by streams and overlain by alluvial sediment deposits and terraces. The interpolated saturated thickness raster resulting from this method did not make physical sense when compared with the elevation dataset.

Ultimately, the saturated thickness was manually input, instead of derived from field data. The Multiple Ring Buffer tool was used to delineate several zones at the following distances from the stream flowlines: 5m, 10m, 30m, 100m, 200m, and 3,000m. These zones have saturated thicknesses of: 1m, 3m, 6m, 10m, 12m, and 20m, respectively. This approach is consistent with the conceptual understanding of the floodplain conveyance system depicted in Figure 2, as alluvium depth generally increases with lateral distance from the stream. The saturated thickness raster is shown in Figure 4.

### Saturated Thickness Raster

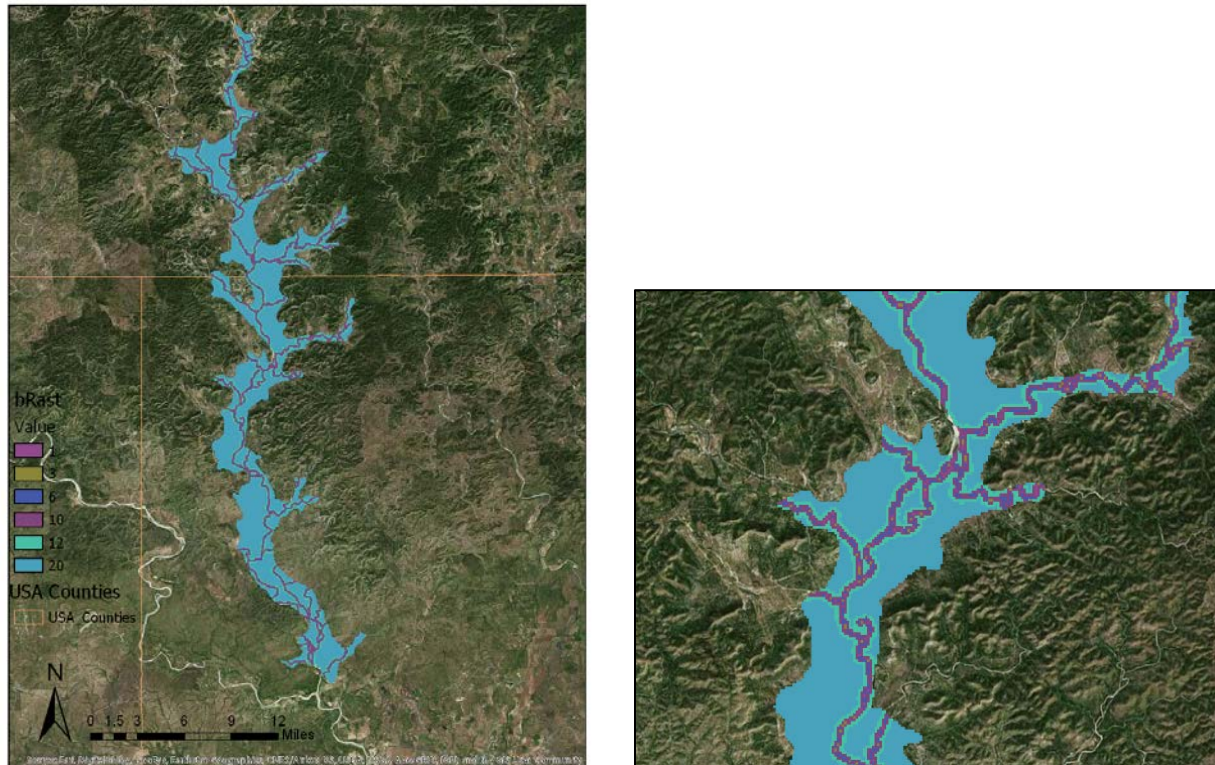


Figure 4. Saturated thickness of alluvium raster, created with the Multiple Ring Buffer tool. A detailed view is at right.



The transmissivity and porosity rasters were determined using the Texas geologic map maintained by the Texas Natural Resources Information System (Figure 5). The alluvial units were delineated from the geologic map and are listed in Table 1 along with reasonable estimates of formation hydraulic conductivity and porosity.

Table 1. Hydraulic conductivity and porosity by geologic unit.

Unit	Description	K (m/s)	Porosity (unitless)
Qt and Qle	Terrace sand	$10^{-4}$	0.3
Qal	Sand and silt	$10^{-7}$	0.37
Qu	Sand and silt	$10^{-7}$	0.4
Kdvr and Kgr	Limestone	$10^{-8}$	0.1

### Geologic Units in Nueces Floodplain

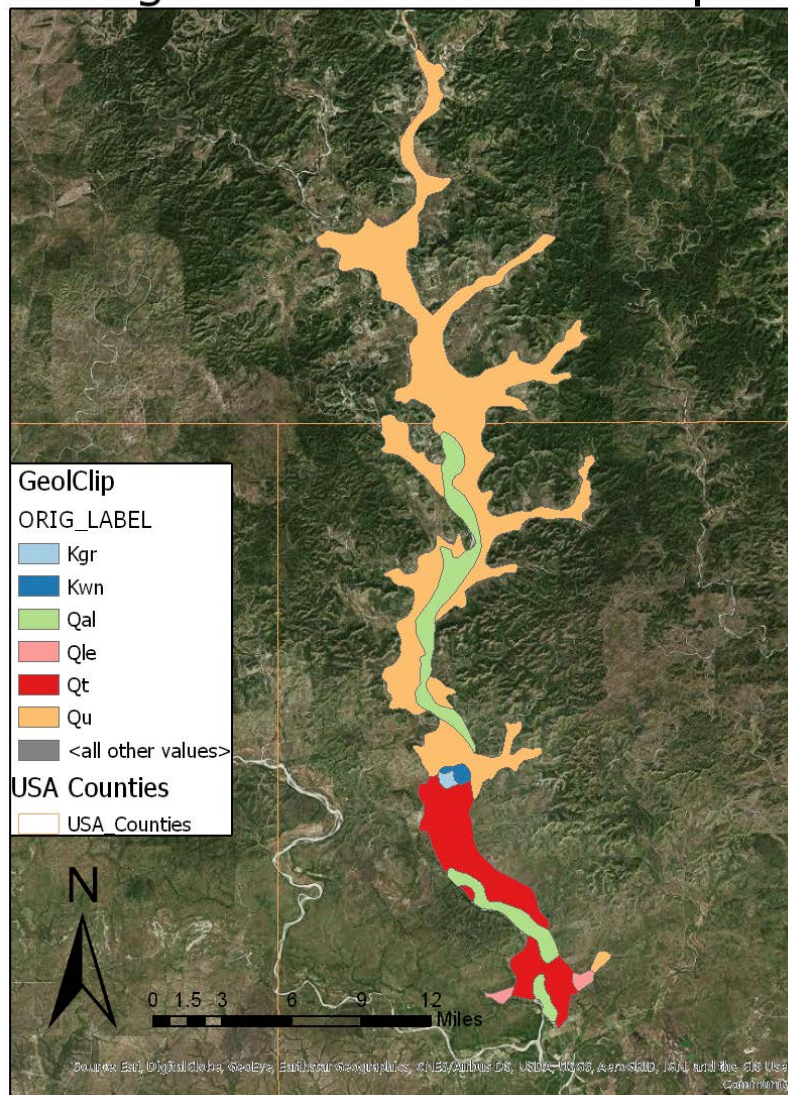


Figure 5. The geologic units within the upper Nueces River basin. The extents of the alluvial units shown above were considered to be the extent of the floodplain. All of the raster inputs to the Darcy Flow tool are this shape.



# Hydraulic Conductivity in Nueces Floodplain

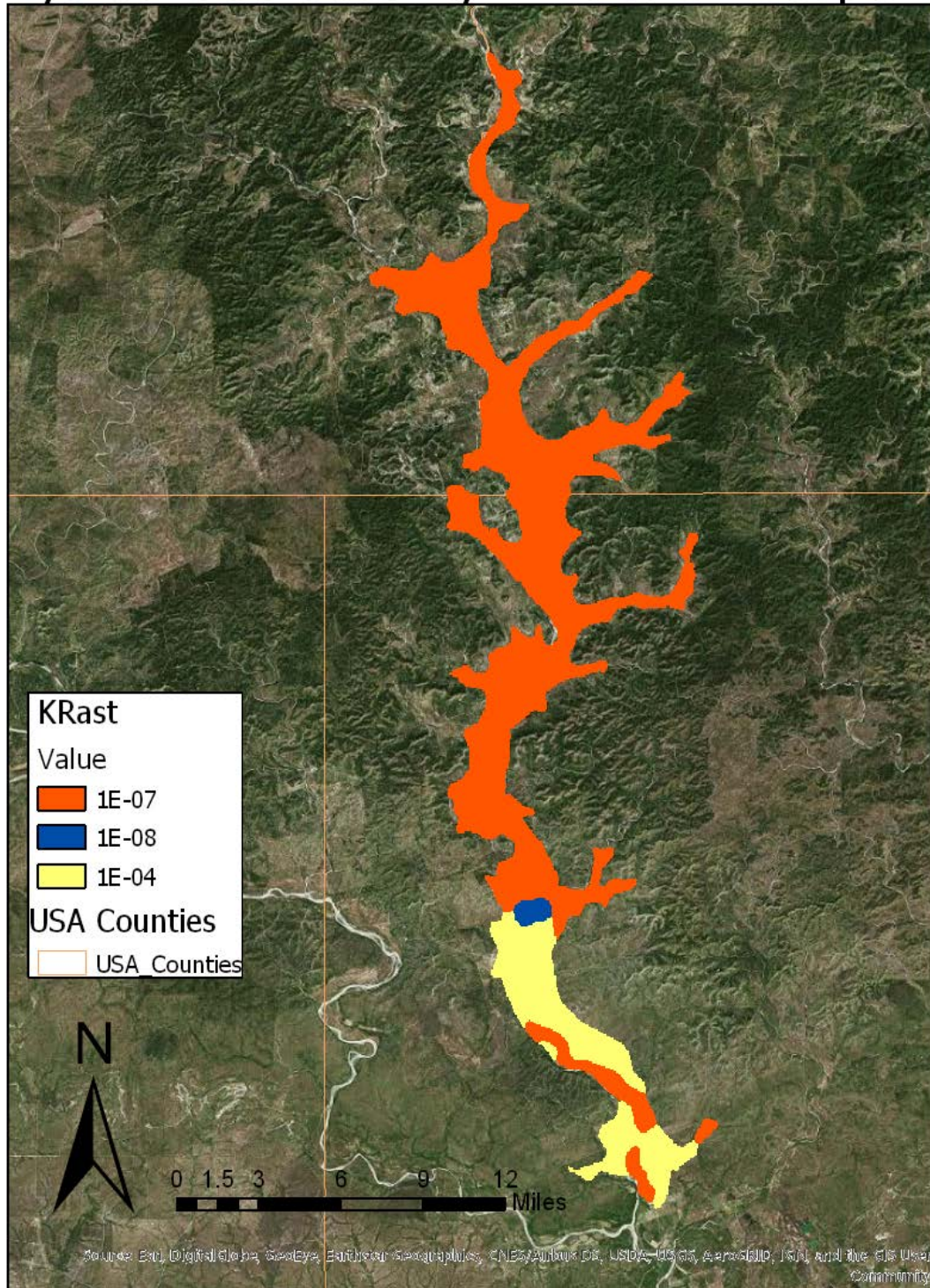
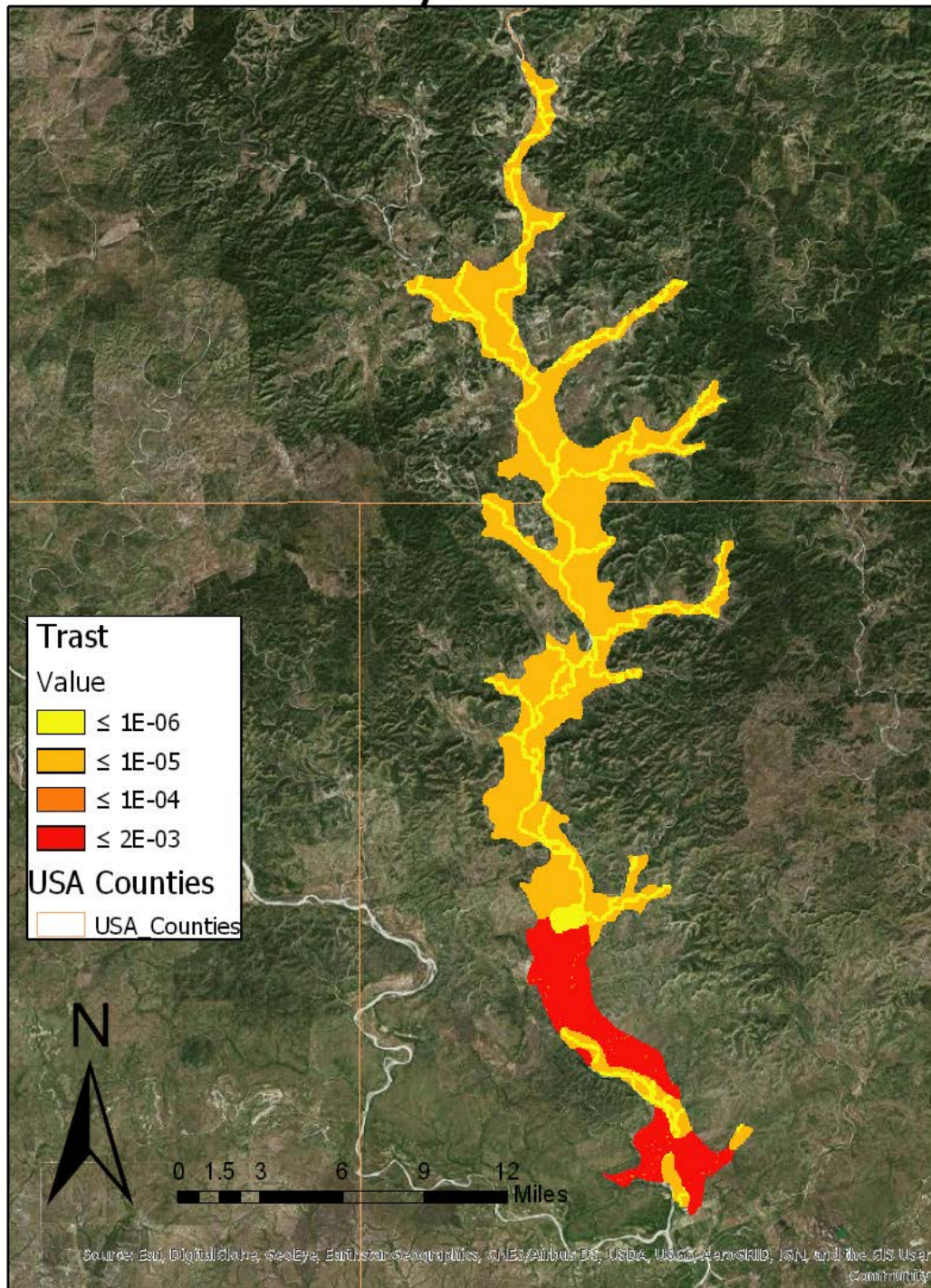


Figure 6. Hydraulic conductivity (K) raster in the upper Nueces River basin. Values correspond to average numbers for the geologic units in Figure 5.



# Transmissivity Raster



*Figure 7.* Transmissivity raster within the upper Nueces River floodplain. Transmissivity is equal to the hydraulic conductivity,  $K$ , multiplied by the saturated thickness,  $b$ . Hydraulic conductivity varies by geologic unit (Figures 5 and 6) and saturated thickness varies by lateral distance from the streamline (Figure 4).



# Porosity of Alluvial Units in Nueces Floodplain

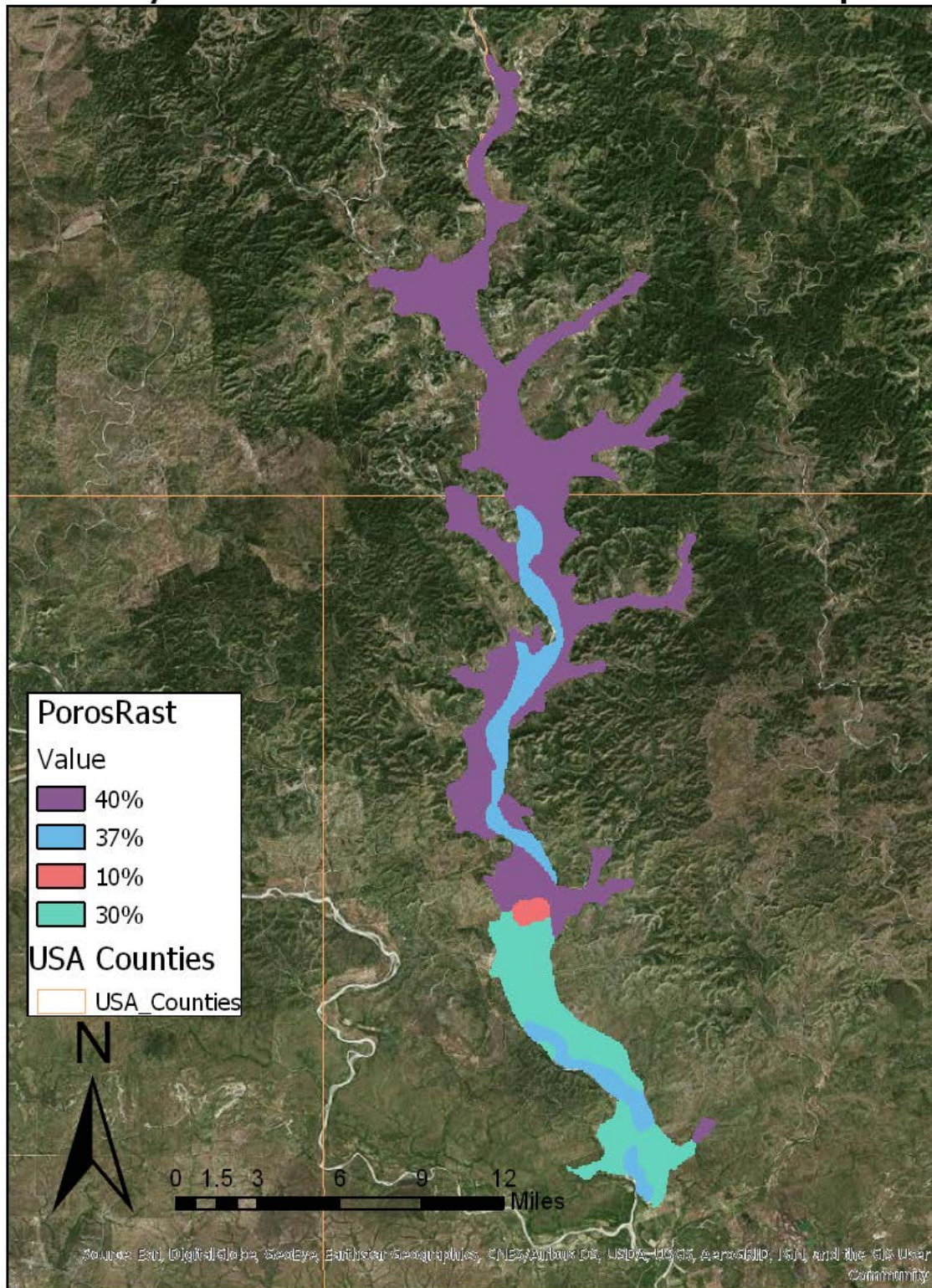


Figure 8. Porosity of the alluvial units in the upper Nueces River floodplain. These are average values for the geologic units shown in Figure 5.



**Results**

The upper Nueces River basin, called the headwaters watershed, was delineated in ArcGIS Pro using the National Hydrography Dataset (NHD Plus). Tables 2 and 3 contain basic watershed and subbasin characteristics. The headwaters watershed has relatively low flows (only 203 cfs at the downstream point, as calculated in ArcGIS), which vary greatly throughout the year. The most upstream reaches drain canyon-like hillslopes, which flatten out rapidly as the river flows into Uvalde County. The Darcy Flow calculation was performed on a raster set that corresponds to the geologic units mapped in this region. The areal extent of those rasters are smaller than the watershed delineated in Figures 9 and 10.

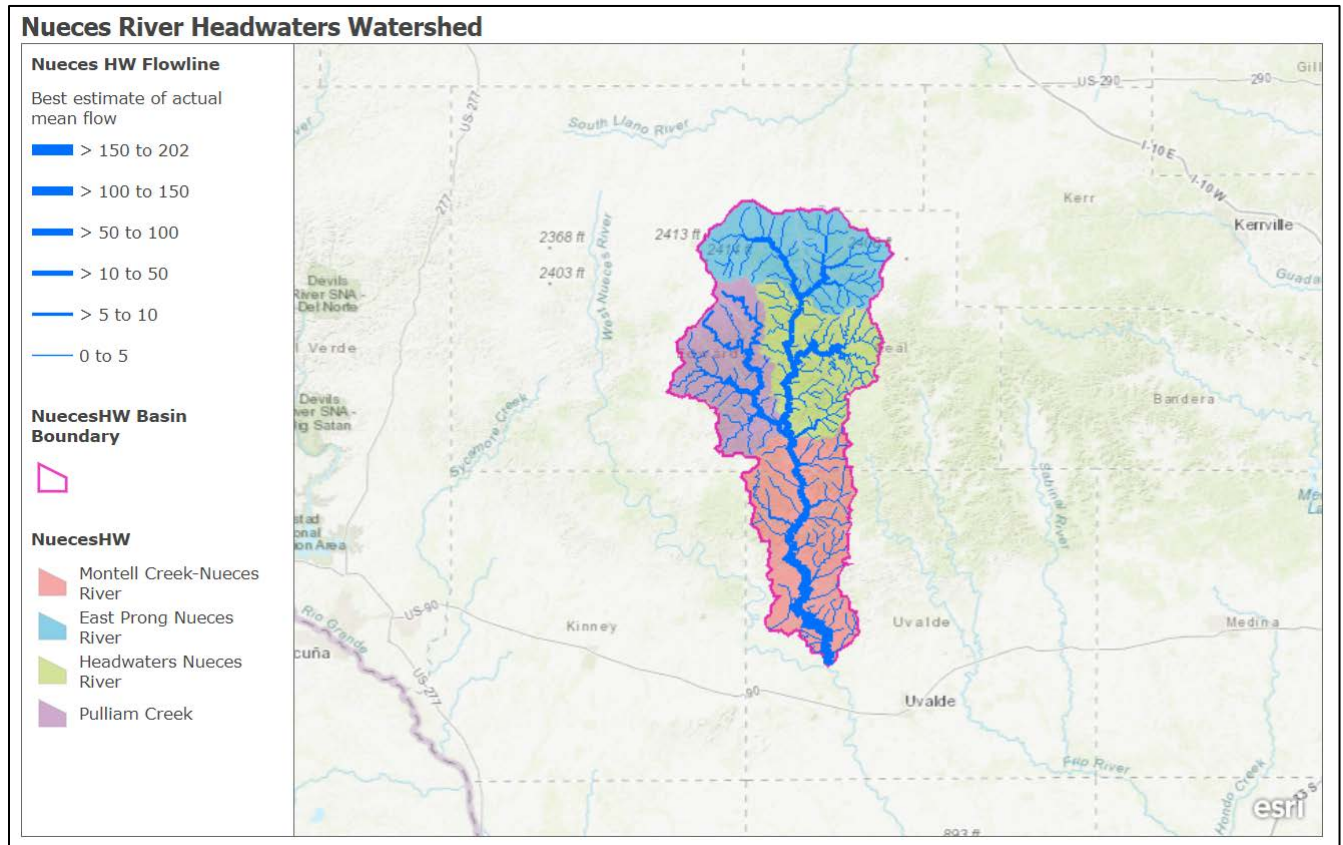


Figure 9. The Nueces River Headwaters Watershed, as delineated using the National Hydrography Dataset.

Table 2. Basic watershed characteristics calculated for the Nueces River Headwaters watershed.

	km or km <sup>2</sup>	mi or mi <sup>2</sup>	Amount
<b>Total area of Nueces HW Subbasin- sum of catchment areas (mi<sup>2</sup>)</b>	2115.9	817.0	
<b>Total area of Nueces HW Subbasin- most downstream flowline (mi<sup>2</sup>)</b>	2115.1	816.6	
<b>Total area of Nueces HW Subbasin- from Q#1 (mi<sup>2</sup>)</b>		816.7	
<b># of NHDPlus catchments in Nueces HW Subbasin</b>			489
<b>Avg area of NHDPlus catchments (mi<sup>2</sup>)</b>	4.3	1.7	

<b># of NHDPlus flowlines in Nueces HW Subbasin</b>			493
<b>Avg length of NHDPlus flowlines in Nueces HW Subbasin (mi)</b>	2.5	1.6	
<b>Total length of NHDPlus flowlines in Nueces HW Subbasin (mi)</b>	1235.7	767.8	
<b>Best est. of actual mean flow at outlet of Nueces HW Subbasin (cfs)</b>			203.0
<b>Average slope of flowlines in Nueces HW Subbasin</b>			-81.1

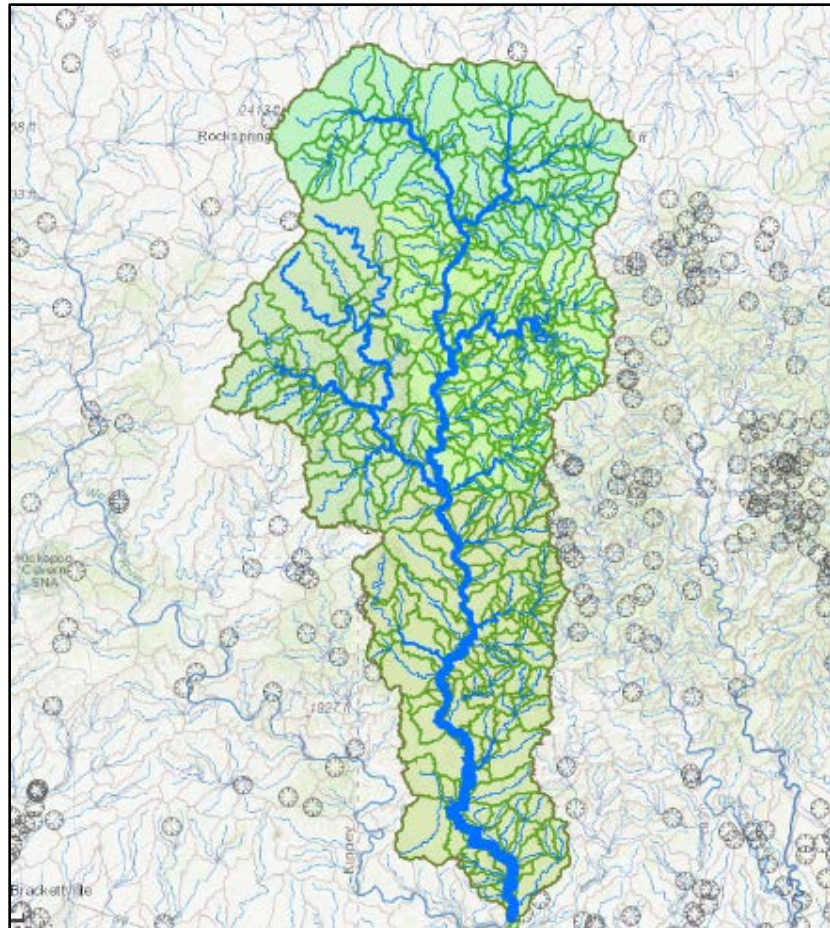


Figure 10. The subbasins within the Nueces River Headwaters watershed.

Table 3. Subbasin characteristics.

	<b>acres</b>	<b>mi<sup>2</sup></b>	<b>Amount</b>
<b>Area of Nueces HW Subbasin (mi<sup>2</sup>)</b>	522714.0	816.7	
<b># of HUC12 subwatersheds in Nueces HW Subbasin</b>			21
<b>Avg area of HUC12 subwatersheds (mi<sup>2</sup>)</b>	24891.0	38.9	
<b># of HUC10 watersheds in Nueces HW Subbasin</b>			4
<b>Avg area of HUC10 watersheds (mi<sup>2</sup>)</b>	24756.2	38.7	



The results of the Darcy Flow tool are three rasters describing the magnitude and direction of subsurface porous medium flow as well as a raster of the residuals from the water balance within each cell. Figures 11 through 13 show these results.

## Magnitude of Darcy Flow Through Alluvium

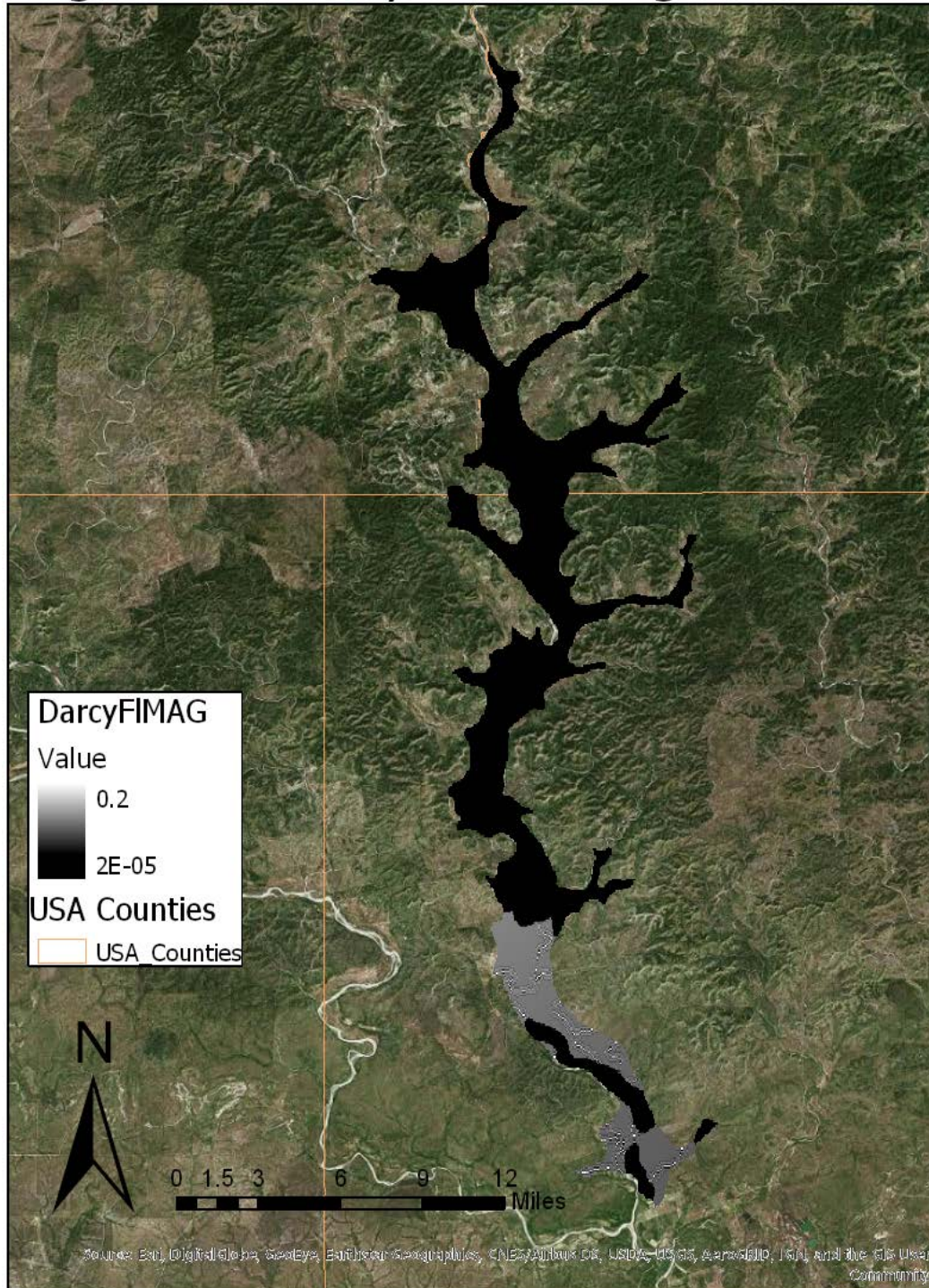


Figure 11. Magnitude of Darcy flow (seepage velocity) through alluvium in the Nueces basin.



# Magnitude of Darcy Flow Through Alluvium

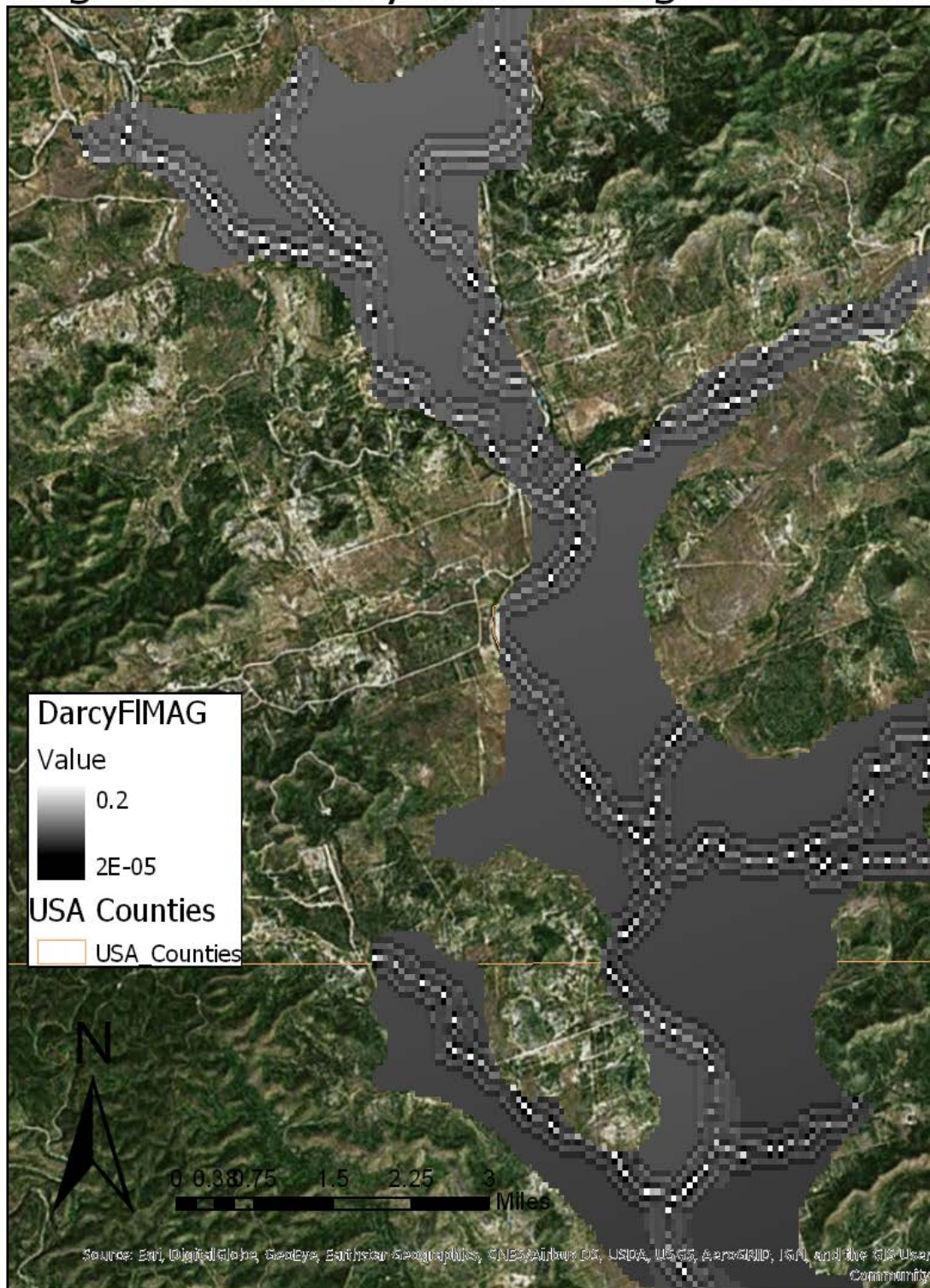
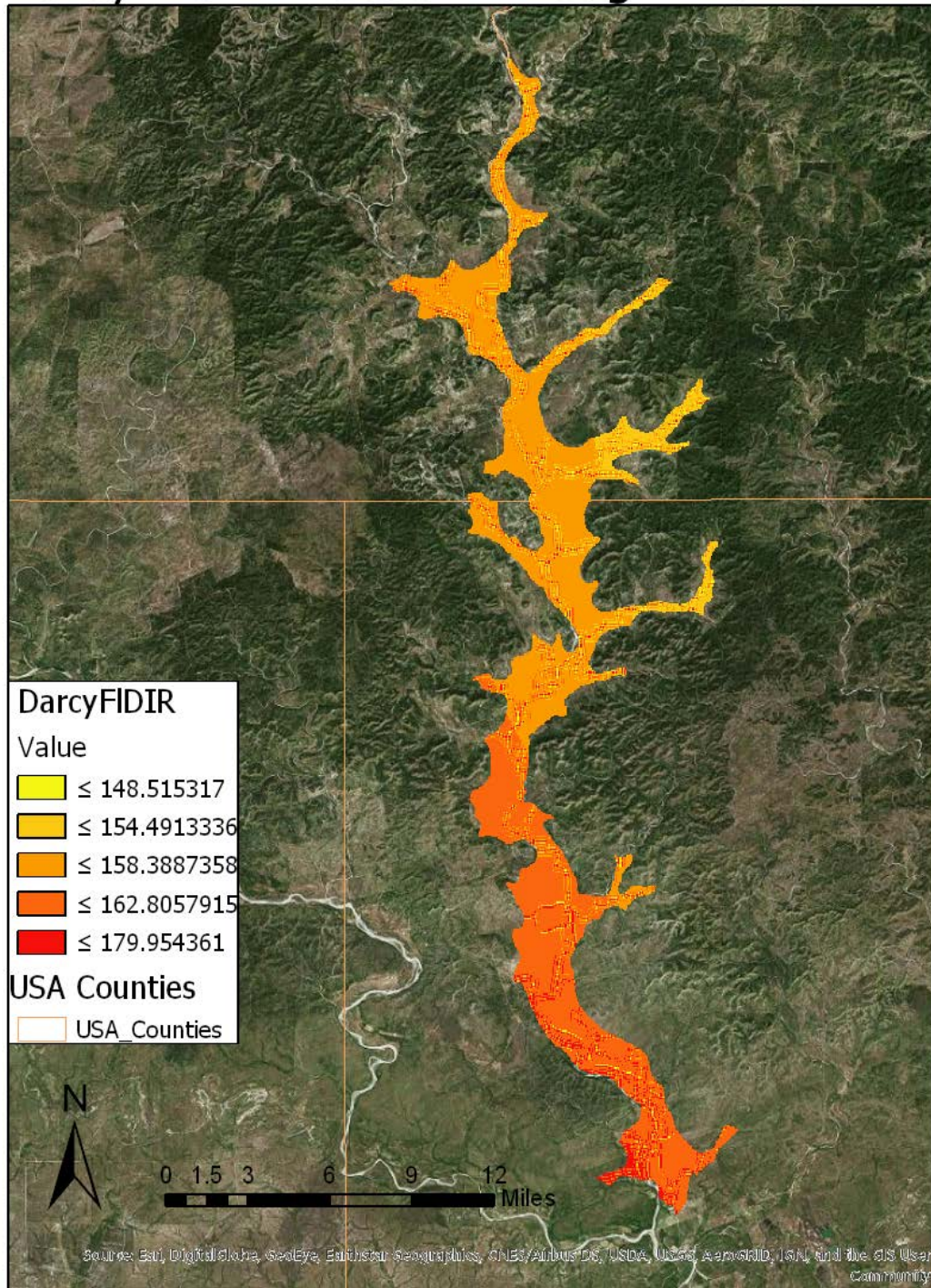


Figure 12. Detailed view of the seepage velocity in the upper reaches of the basin. The highest velocities are closest to the stream.



## Darcy Flow Direction Through Alluvium



*Figure 13.* Darcy flow direction through the alluvium. The groundwater generally flows towards the southeast, in the direction of the groundwater head gradient. Locally around the streambed, the groundwater flows in a more southerly direction. This agrees with the conceptual model of flow in the watershed.



# Volume Balance Residual for Darcy Flow Tool

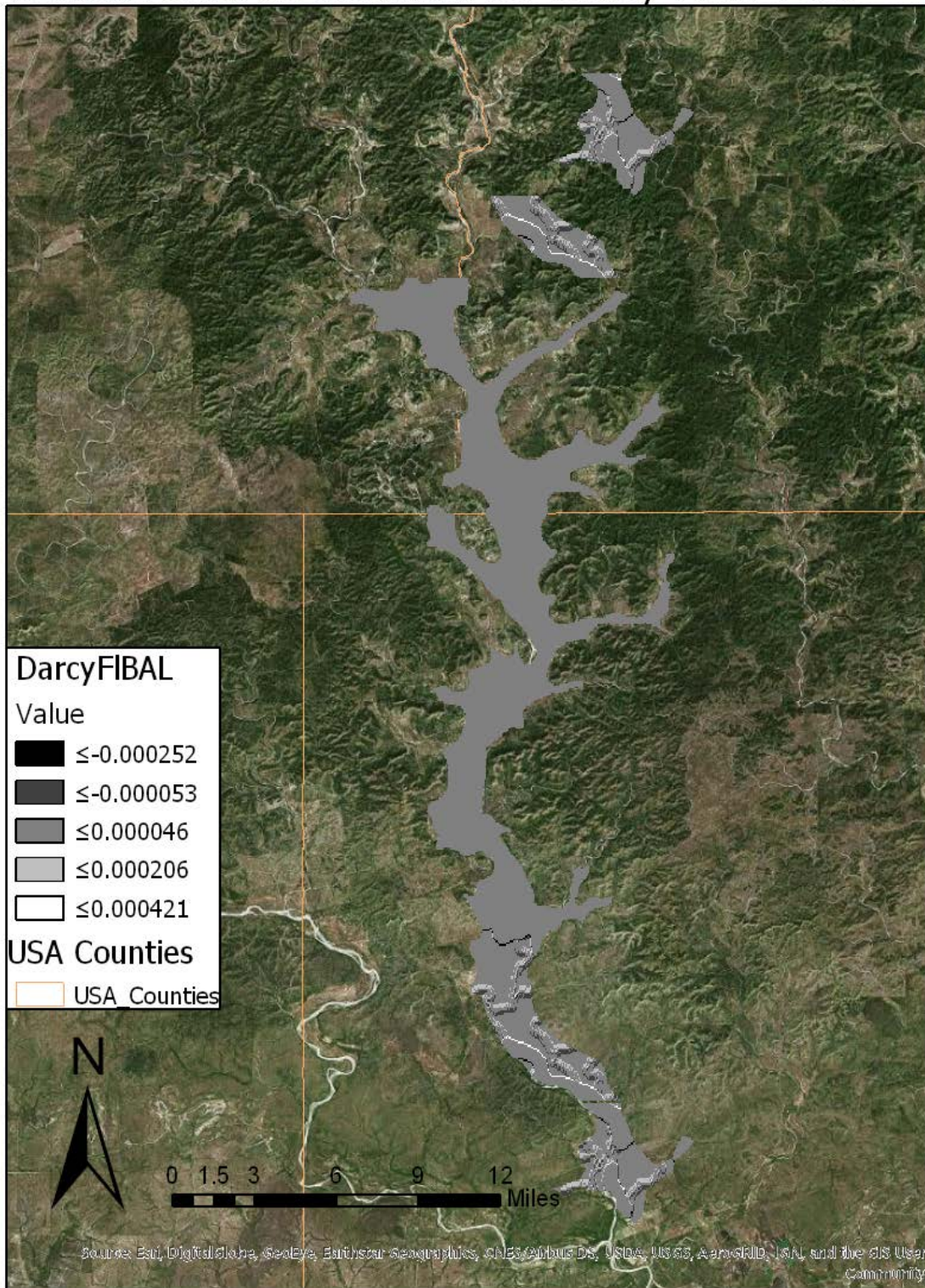


Figure 14. The volume balance residual as calculated by the Darcy Flow tool. The tool accurately balanced the subsurface flow through each cell.



**Discussion**

The subsurface flow magnitude calculated with the Darcy Flow tool agrees well with field data collected in March 2017 using dye tracer testing. Fluorescent dye tracer tests are used to delineate subsurface flowpaths and estimate subsurface velocities. They are especially useful in karstic systems, such as the upper Nueces, where shallow groundwater could flow through alluvium and enter a karstic conduit in the underlying bedrock.

**Potential Flowpaths between Dye Injection Point and CAN012**

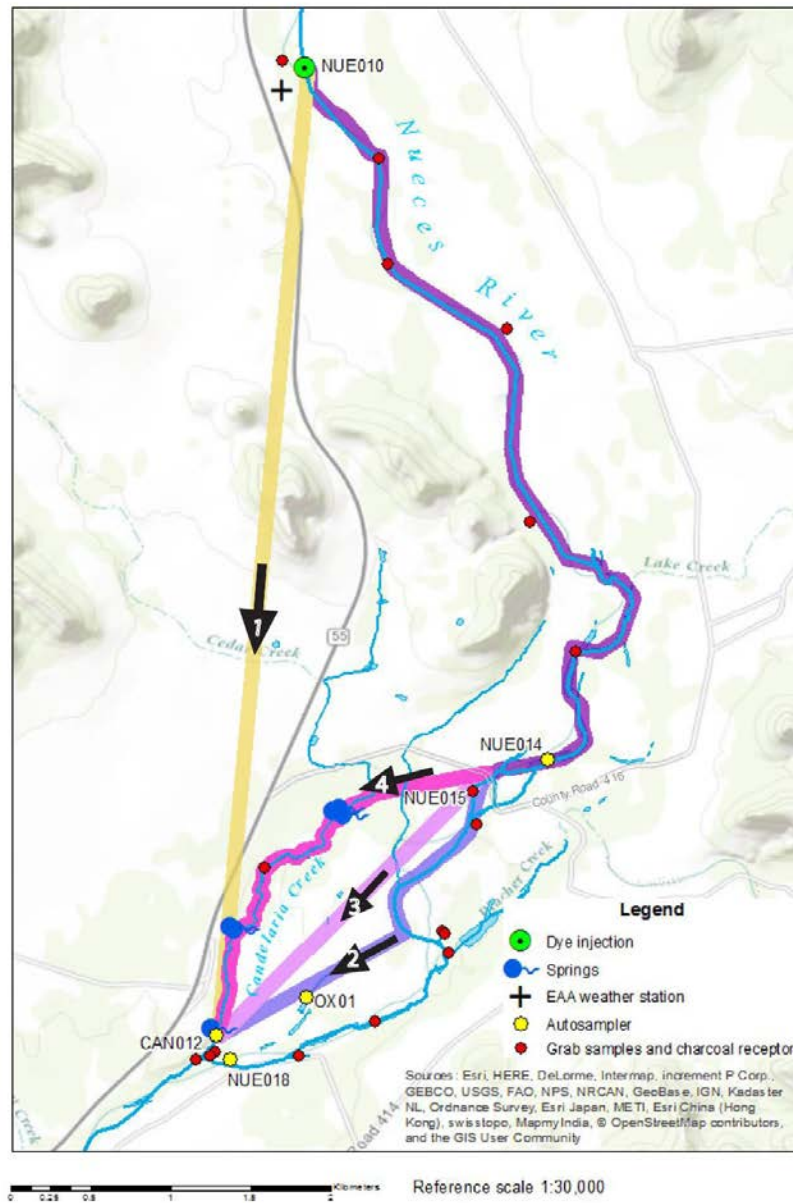


Figure 15. Fluorescent uranine dye was injected into the Nueces River at site NUE010 at the top of the map. The dye was detected at the downstream end of a creek at site CAN012 at the bottom of the figure. The dye is hypothesized to have taken one of the four flowpaths marked in yellow, magenta, pink, and purple.

*Table 4.* Subsurface velocities calculated for the four hypothesized flowpaths shown in Figure 15. These velocities are similar to the seepage velocities found using the Darcy Flow tool.

<b>Path</b>	<b>Description</b>	<b>Apparent velocity through subsurface portion of path (m/s)</b>	<b>Total flowpath length (m)</b>
1	Straight-line path through subsurface from NUE010 to CAN012	0.016	6142
2	Along river from NUE010 to abandoned oxbow, straight path through subsurface to CAN012	0.0035	8529
3	Along river from NUE010 to NUE015, straight path through subsurface to	0.0065	8359
4	Along river from NUE010 to NUE015, straight path through subsurface to CAN002, along Candelaria Creek to CAN012	<0.0035	8908



*Figure 16.* Uranine dye immediately downstream of the injection point on the Nueces River, March 2017. The non-toxic, fluorescent dye is used to investigate subsurface velocities.



The Darcy Flow tool calculated subsurface velocities ranging from  $2E-5$  m/s to 0.2 m/s. These values agree remarkably well with the velocities listed in Table 4, which were calculated from dye tracer testing on the Nueces. As shown in Figure 12, the seepage velocity is generally fastest in cells close to the streamlines, which is what is expected based on the conceptual understanding of the floodplain conveyance system. The alluvium deposited directly in the streambeds is generally well-sorted, cobble-sized gravel with very high K and T values. Older terraces are generally composed of lenses of gravels, sands, and sandy gravels, with lower porosity due to compaction.

The Nueces basin is a karstic system, meaning the alluvium is likely underlain by karstic conduits and fractures that could drain shallow groundwater from the alluvium and in some instances could input water into the alluvium, as is the case at several known springs and seeps. This simple model completed in this study does not account for these mechanisms. The Darcy Flow tool also does not take into account the high level of heterogeneity among alluvial deposits in the floodplain. The porosity and hydraulic conductivity values were assigned based on the geologic unit, however, there are large variations in these properties even within the same unit and within the same terrace.

Finer resolution data could greatly improve these calculations. As mentioned in the Methods section, several attempts were made to create groundwater elevation and bedrock elevation rasters based on actual field data. These could have been used to create a finer resolution saturated thickness raster. However, well logs and monitoring wells are non-existent within the 5m buffer of streamlines in this region, and a simple stepped-terrace geometry was imposed using concentric buffers.

The Particle Track tool was used to model flowpaths from the dye injection point from the March 2017 field study. The particle path followed the regional groundwater gradient to the southeast, and could not match the local subsurface flowpaths closest to the river, which we know transmit river underflow downstream.

## Particle Track Analysis for Dye Tracer Test

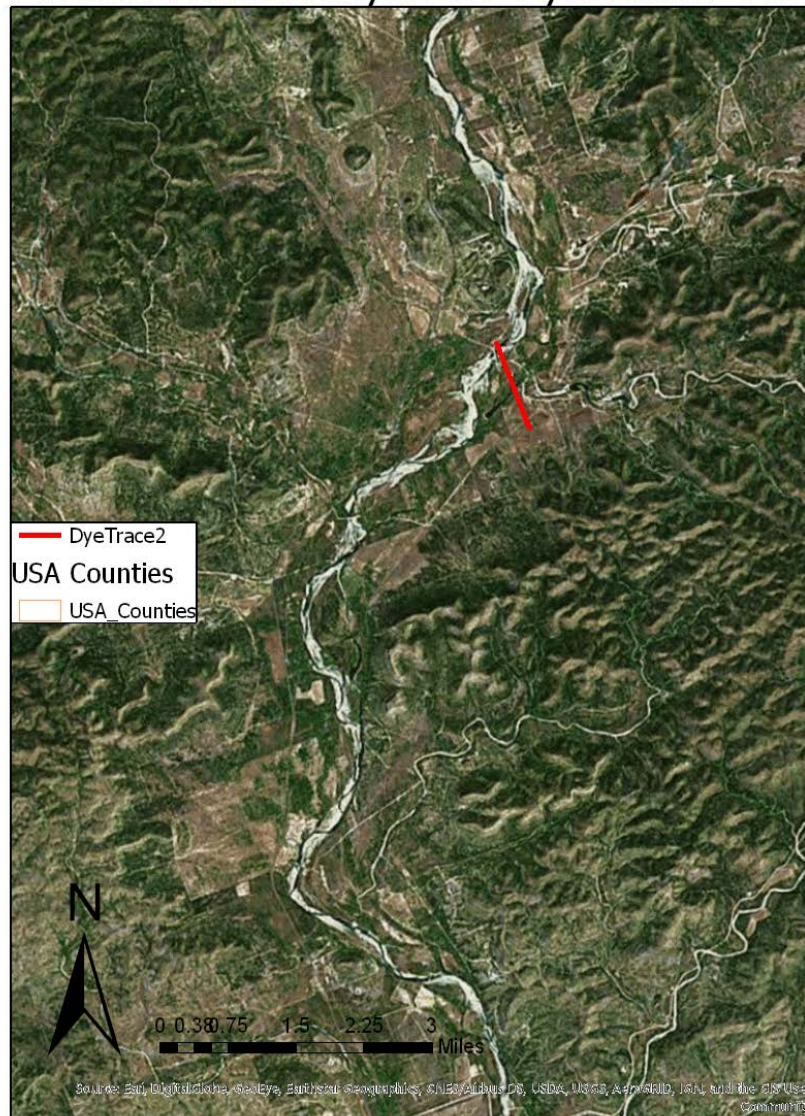


*Figure 17.* Particle Track tool analysis for subsurface flow paths at the dye injection point. This does not agree with observations of dye.

### **Conclusion**

The Darcy Flow tool in ArcGIS Pro can accurately model the subsurface flow through the alluvial floodplain. Despite a limitation in available groundwater data and a coarse resolution geologic map, the subsurface velocities calculated in ArcGIS agree with field estimates. Improvements can be made based upon grain size analysis of samples from throughout the headwaters watershed, which could be used to improve the hydraulic conductivity and porosity inputs. The Particle Track tool, however, could only recreate regional flowpaths, and did not successfully convey the nature of local subsurface flow adjacent to the stream.



## **References**

- Bailly-Comte, V., Borrell-Estupina, V., Jourde, H., and Pistre, S., 2012, A conceptual semidistributed model of the Coulazou River as a tool for assessing surface water-karst groundwater interactions during flood in Mediterranean ephemeral rivers: *Water Resources Research*, v. 48, p. 1–14.
- Batelaan, O., and De Smedt, F., 2007, GIS-based recharge estimation by coupling surface-subsurface water balances: *Journal of Hydrology*, v. 337, p. 337–355.
- Chen, X., Zhang, Y., Zhou, Y., and Zhang, Z., 2013, Analysis of hydrogeological parameters and numerical modeling groundwater in a karst watershed, southwest China: *Carbonates and Evaporites*, v. 28, p. 89–94.
- Chenini, I., and Ben Mammou, A., 2010, Groundwater recharge study in arid region: An approach using GIS techniques and numerical modeling: *Computers and Geosciences*, v. 36, p. 801–817.
- Fleckenstein, J.H., Krause, S., Hannah, D.M., and Boano, F., 2010, Groundwater-surface water interactions: New methods and models to improve understanding of processes and dynamics: *Advances in Water Resources*, v. 33, p. 1291–1295.
- Graf, R., and Przybyłek, J., 2014, Estimation of shallow groundwater recharge using a GIS-based distributed water balance model: *Quaestiones Geographicae*, v. 33, doi: 10.2478/quageo-2014-0027.
- Green, R.T., Winterle, J.R., and Prikryl, J.D., 2008, Discharge from the Edwards Aquifer through the Leona River floodplain, Uvalde, Texas: *Journal of the American Water Resources Association*, v. 44, p. 887–901.
- Hauwert, N.M., 2016, Stream recharge water balance for the Barton Springs segment of the Edwards Aquifer: *Journal of Contemporary Water Research and Education*, p. 24–49.
- Jukić D. and Denić-Jukić, V., 2009, Groundwater balance estimation in karst by using a conceptual rainfall–runoff model: *Journal of Hydrology*, v. 373, p. 302–315.
- Kresic, N. and Mikszewski, A., 2013, *Hydrogeological conceptual site models: data analysis and visualization*: Boca Raton, FL, CRC Press, 584 p.
- Zampieri, M., Serpetzoglou, E., Anagnostou, E.N., Nikolopoulos, E.I., and Papadopoulos, A., 2012, Improving the representation of river-groundwater interactions in land surface modeling at the regional scale: Observational evidence and parameterization applied in the Community Land Model: *Journal of Hydrology*, v. 420–421, p. 72–86.